Chinese Chemical Letters 32 (2021) 2155–2158

Contents lists available at ScienceDirect

Chinese Chemical Letters

journal homepage: www.elsevier.com/locate/cclet

Communication

Sm-doped g-C_3N_4/Ti_3C_2 MXene heterojunction for visible-light photocatalytic degradation of ciprofloxacin

Mingchuan Yu, Huanjing Liang, Ruonan Zhan, Lei Xu, Junfeng Niu*

Research Center for Eco-environmental Engineering, Dongguan University of Technology, Dongguan 523808, China

ARTICLE INFO

Article history:
Received 10 October 2020
Received in revised form 4 November 2020
Accepted 30 November 2020
Available online 4 December 2020

Keywords:
g-C_3N_4
Sm-doped
Ti_3C_2 MXene
Visible light photodegradation

ABSTRACT

A heterojunction of Sm-doped g-C_3N_4/Ti_3C_2 MXene (SCN/MX) was constructed *via* prepolymerization and solid mixture-calcination method. The modified g-C_3N_4 presented a hollow porous seaweed-like shape which can increase its specific area and active sites. In SCN/MX composite, the optical properties, no matter optical absorption ability or separation performance of photo-induced electrons and holes, were enhanced. Among them, Sm-doping may play an important role on transferring the photogenerated electrons to suppress their recombination, and Ti_3C_2 MXene would broaden light absorption and further improve the carrier migration efficiency. The SCN/MX presented higher photocatalytic degradation efficiency (> 99%) of ciprofloxacin under visible light irradiation. The quenching experiments and electron spin-resonance spectroscopy confirmed that the dominated active materials were superoxide radical and holes. The degradation mechanisms of ciprofloxacin (CIP) over the SCN/MX were attacking of the active materials on the piperazine ring and quinolone ring, and the final products were CO_2, H_2O and F^-.

Ciprofloxacin (CIP) is a typical representative of fluoroquinolone antibiotics, which is often used in the diseases treatment of human and pets. CIP in the environment mainly comes from the wastewaters of hospitals, pharmaceutical industry and animal farms. Studies have found that only 30%–70% of the parent compounds of fluoroquinolone antibiotics are metabolized in the human body, and if they discharge into the sewage treatment plant, the antibiotics cannot be completely removed [1,2]. Moreover, studies also have shown that there are more than ten kinds of metabolites in the conversion process of CIP, and these metabolites bring potential risks to the environment and even to humans [3,4]. Considering high efficiency degradation, feasible technology and reasonable cost, photocatalysis has drawn more and more attention recently. Especially, fluoroquinolones are compounds susceptible to photodegradation process compared to other advanced oxidation technologies [5]. Graphitic carbon nitride (g-C_3N_4) is a non-metallic photocatalytic material, and it has been developed for photocatalytic water splitting by Wang *et al.* in 2009 [6]. Even though it has been widely studied in photocatalysis fields [7–9], g-C_3N_4 itself also has disadvantages such as easy agglomeration during synthesis process, easy recombination of photo-generated electrons and holes, poor conductivity and low light absorption, which limit its development and application.

To solve the above problems, we prepared g-C_3N_4 *via* prepolymerization method for reducing the agglomeration and increasing specific area and active sites [10,11]. Furthermore, metal ions doping and heterojunction construction have been the main ways to enhance the photocatalytic activity [12,13]. The rare earth metal ions doping into g-C_3N_4 can effectively depress photo-generated electron-hole pairs recombination because of its unique unfilled 4f orbital and empty 5d orbital [14]. Moreover, the CN-based heterojunction with two-dimensional (2D) material is suggested to be the optimal contact style because it displays the highest surface contact interface [15,16]. 2D sheet material Ti_3C_2 MXene was discovered in 2011 [17]. MXenes possess hydrophilic surface and high metallic conductivities which makes it show promising performance in electrocatalysis, photocatalysis, energy storage devices and other applications [18].

Herein, we prepared g-C_3N_4 (CN) *via* prepolymerization method and constructed a heterojunction photocatalyst, Sm-doped g-C_3N_4/Ti_3C_2 MXene (SCN/MX) (Table S1 in Supporting information). The morphologies, components and structure of the prepared SCN/MX samples were characterized. The optical properties, including optical absorption ability and separation performance of photo-induced electrons-holes were analyzed after introducing of Sm-doping and MXene. These special structures and improved optical properties were beneficial to enhance photocatalytic activity for CIP degradation. The band

* Corresponding author.
E-mail address: niujf@dgut.edu.cn (J. Niu).

https://doi.org/10.1016/j.cclet.2020.11.069

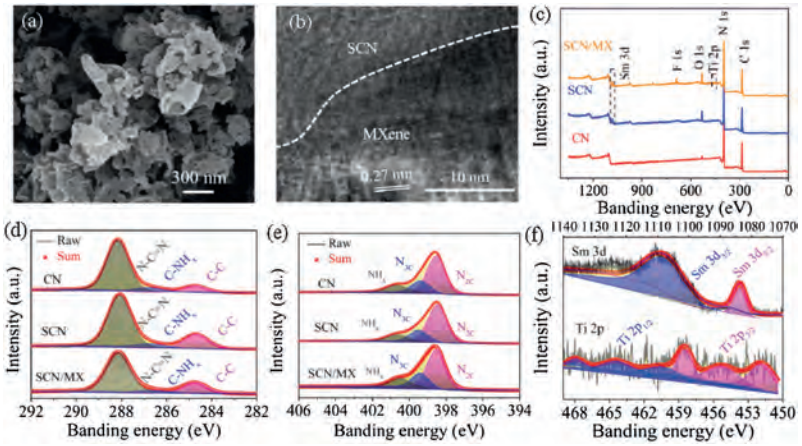

Fig. 1. (a) SEM, (b) HRTEM, (c) survey XPS spectra, (d) C 1s XPS spectra, (e) N 1s XPS spectra and (f) Sm 3d and Ti 2p XPS spectra of the SCN/MX, herein the component of the SCN/MX was $S_{0.01}CN/MX_{0.01}$.

structure of the SCN/MX and its degradation mechanism and pathway under visible light irradiation were discussed.

SCN/MX was prepared *via* prepolymerization and solid mixture-calcination method [19]. The morphology of the SCN/MX presented a hollow porous seaweed-like shape from scanning electron microscopy (SEM) (Fig. 1a). These structures provided more specific surface areas and active sites which can in favor of enhancing photocatalytic activity, compared to traditional sheet-like CN (Figs. S1 and S2 in Supporting information). The heterojunction structure of SCN/MX was proved by high resolution transmission electron microscopy (HRTEM). In Fig. 1b, an obvious interface structure between CN and MX was observed [20]. The lattice spacing of 0.27 nm was ascribed to the plane of MXene [21]. Further, the SCN/MX was characterized by X-ray photoelectron spectroscopy (XPS). Compared to pure CN, the existence of Sm 3d, F 1s, and Ti 2p presented that the SCN/MX was formed successfully (Fig. 1c). Among them, F 1s was ascribed to the F* that terminated MXene surface during preparation. The C 1s XPS spectra for pristine CN, SCN and SCN/MX contained three components corresponding to standard carbon (284.7 eV), C-NH_x on the edges of heptazine units (286.8 eV) and N—C= N coordination in the framework CN (288.2 eV) (Fig. 1d). The N 1s XPS spectra of the three samples were deconvoluted into three peaks located at 398.6, 400.4 and 401.0 eV, corresponding to bicoordinated nitrogen (N_{2C}), tricoordinated nitrogen (N_{3C}) and NH_x groups in the heptazine framework, respectively (Fig. 1e) [22,23]. For SCN/MX, it contained Ti 2p and Sm 3d XPS spectra (Fig. 1f). The peaks at 452–458 eV and 460–468 eV in Ti 2p XPS spectra were belong to Ti $2p_{3/2}$ and Ti $2p_{1/2}$, respectively [24,25]. The peaks located at 1082.9 and 1105.1 eV were assigned to Sm $3d_{5/2}$ and Sm $3d_{1/2}$, respectively, indicating that Sm^{3+} existed [26,27]. Moreover, the C/N ratio of the SCN (0.90) and SCN/MX (0.88) increased compared to the pristine CN (0.81) from XPS spectra, demonstrating that the materials component changed after doping Sm [28].

The optical properties, including optical absorption ability and separation performance of photo-induced electrons and holes were carried out by diffuse reflectance spectra (DRS), photoluminescence (PL) emission spectra, photocurrent response and electrochemical impedance spectroscopy (EIS). In Fig. 2a, the CN/MX and SCN/MX both exhibited wider absorption edge compared to the pristine CN, suggested that the introduced MX can improve the visible light response. The corresponding band gap energy was calculated in Fig. 2b. The PL responses of the various Sm-doped dosages and MXene dosages are shown in Figs. 2c and d, respectively. Compared with the pristine CN, all SCN/MX samples presented the PL signals with a relative low intensity, indicated that the recombination of photoexcited electrons and holes was weaken [29]. Moreover, the photocurrent density of the SCN/MX

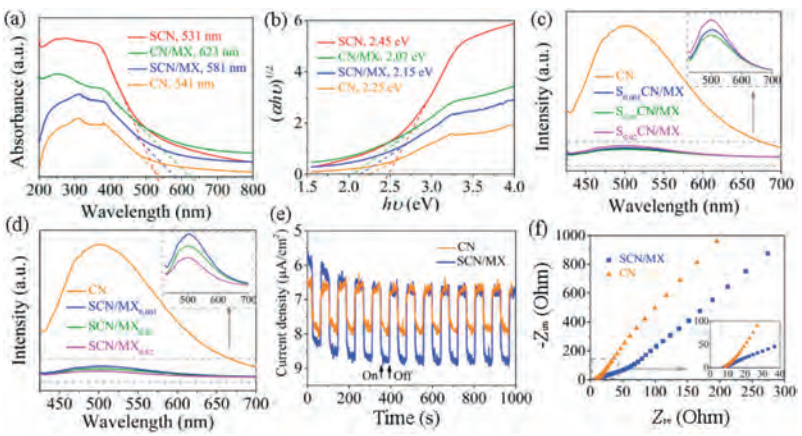

Fig. 2. (a) UV–vis DRS absorption spectra, (b) plots of transformed Kubelka-Munk function *versus* photon energy, (c, d) PL spectra, (e) photocurrent response and (f) Nyquist plot from EIS of the samples.

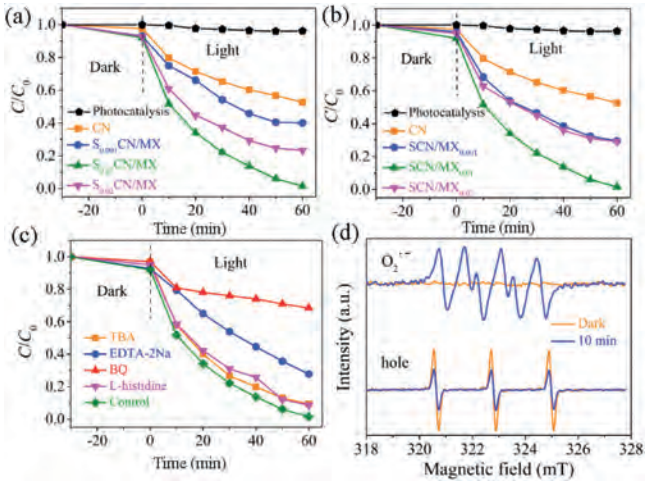

Fig. 3. (a) Photocatalytic degradation of CIP using CN and SCN/MX samples with various Sm-doping dosages. (b) Photocatalytic degradation of CIP using CN and SCN/MX samples with various MXene dosages. (c) Quenching experiments and (d) ESR of the $S_{0.01}CN/MX_{0.01}$.

was higher than that of the pristine CN (Fig. 2e), whereas the semicircle diameter of the SCN/MX was smaller than that of the pristine CN (Fig. 2f). All these results indicated that higher photocatalytic activity of the SCN/MX was ascribed to the doped Sm and introduction of MXene [30].

Photocatalytic degradation performance of CIP over the SCN/MX was carried out. Figs. 3a and b show the photocatalytic degradation over SCN/MX with various Sm-doped dosages and MXene dosages, respectively. All SCN/MX samples presented better photocatalytic activity compared to pristine CN. The optimal component in SCN/MX was $S_{0.01}CN/MX_{0.01}$, and its photocatalytic degradation efficiency was over 99% during 60 min. Combined the above results of optical properties, it was speculated that Sm-doping may play an important role on transferring the photogenerated electrons to suppress their recombination, and Ti_3C_2 MXene would broaden light absorption and further improve the carrier migration efficiency. We adopted quenching experiments to identify the reactive species for CIP degradation using p-benzoquinone (BQ), tert-butanol (TBA), L-histidine and ethylenediaminetetraacetic acid disodium (EDTA-2Na) as scavengers for superoxide radical ($O_2^{\bullet-}$), hydroxyl radicals ($^{\bullet}OH$), singlet oxygen ($^1O_2$) and hole (h^+), respectively (Fig. 3c). An obvious suppression phenomenon was observed when BQ and EDTA-2Na were introduced into photodegradation system, suggested that $O_2^{\bullet-}$ and h^+ played important roles during the initial reaction. Simultaneously, we confirmed the experience of the two species *via* electron spin-resonance spectroscopy (ESR) (Fig. 3d). Moreover, the effect of the initial pH value on degradation shows that the optimal degradation efficiency was obtained under neutral pH value, suggested the neutral condition was favor of the active radicals formation (Fig. S3 in Supporting information).

The band structure of the $S_{0.01}CN/MX_{0.01}$ is shown in Fig. 4. The valence band (VB) and conduction band (CB) of the pristine CN were 2.05 and −0.2 eV, respectively. As the pristine CN was excited by visible light, the photoexcited electrons and holes transformed to VB and CB, respectively, and parts of electrons and holes would recombine resulting in reducing its photocatalytic activity. After introducing Sm and MXene, the VB and CB of the $S_{0.01}CN/MX_{0.01}$ were calculated to be 2.00 and −1.27 eV, respectively, which can induce the formation of $O_2^{\bullet-}$ (−0.33 eV). Meanwhile, the formed electrons can be transported *via* the MXene which effectively inhibited the recombination. The generated $O_2^{\bullet-}$ and holes can react with the contaminant CIP. The CIP was decomposed *via* radicals, mainly were $O_2^{\bullet-}$ and holes, attacking on the piperazine ring and quinolone ring, and the final products were CO_2, H_2O and F^- [31,32].

The $S_{0.01}CN/MX_{0.01}$ was constructed with CN, $Sm(NO_3)_3$ and Ti_3C_2 MXene as precursors *via* a solid mixture-calcination method. After addition of rare metal Sm-doping and conductive Ti_3C_2 MXene, the optical absorption range and carriers transformation ability were improved. All these properties made the $S_{0.01}CN/MX_{0.01}$ present higher photocatalytic degradation of CIP under visible light irradiation. It is a promising strategy to construct heterojunction photocatalytic materials for removal of contaminants from waters.

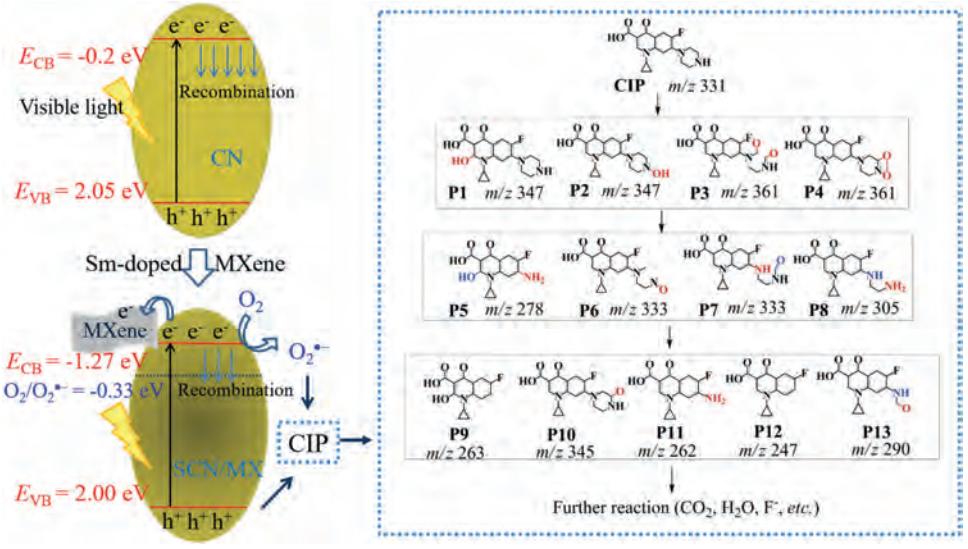

Fig. 4. Proposed photocatalytic mechanism for CIP degradation over SCN/MX under visible light irradiation.

Declaration of competing interest

The authors report no declarations of interest.

Acknowledgments

This study was financially supported by the National Natural Science Foundation of China (No. 51878169), Guangdong Basic and Applied Basic Research Foundation (No. 2019A1515110760), Guangdong Innovation Team Project for Colleges and Universities (No. 2016KCXTD023), and Guangdong Province Universities and Colleges Pearl River Scholar Funded Scheme (2017).

Appendix A. Supplementary data

Supplementary material related to this article can be found, in the online version, at doi:https://doi.org/10.1016/j.cclet.2020.11.069.

References

[1] T. Deng, Y. Ge, C. Tan, et al., Chem. Eng. J. 330 (2017) 1390–1400.
[2] Z. Diao, X. Xu, D. Jiang, et al., J. Hazard. Mater. 327 (2017) 108–115.
[3] X. Wen, C. Niu, L. Zhang, et al., J. Catal. 358 (2018) 141–154.
[4] X. Ao, W. Liu, W. Sun, et al., Chem. Eng. J. 345 (2018) 87–97.
[5] U. Hubicka, P. Zmudzki, P. Talik, et al., Chem. Cent. J. 7 (2013) 1–12.
[6] X. Wang, K. Maeda, A. Thomas, et al., Nat. Mater. 8 (2009) 76–80.
[7] F. Yu, L. Wang, Q. Xing, et al., Chin. Chem. Lett. 31 (2020) 1648–1653.
[8] L. Zhang, H. Liu, et al., Angew. Chem. Int. Ed. 59 (2020) 1–6.
[9] W. Liu, W. Zhang, M. Liu, et al., Chin. Chem. Lett. 33 (2019) 2177–2180.
[10] J. Zhang, X. Chen, K. Takanbe, et al., Angew. Chem. Int. Ed. 49 (2010) 441–444.
[11] C. Zhou, C. Lai, D. Huang, et al., Appl. Catal. B: Environ. 220 (2018) 202–210.
[12] M. Rakibuddin, H. Kim, J. Aolly Compd. 832 (2020) 154887.
[13] C. Jin, W. Li, Y. Chen, et al., Ind. Eng. Chem. Res. 59 (2020) 2860–2873.
[14] Z.N. Kayani, M. Sahar, S. Riaz, et al., Opt. Mater. 108 (2020) 110457.
[15] S. Kumar, V. Sharma, K. Bhattachayya, V. Krishnan, Mater. Chem. Front. 1 (2017) 1093–1106.
[16] H. Liang, H. Peng, Y. Zhou, et al., Chin. Chem. Lett. 30 (2019) 2245–2248.
[17] M. Naguib, M. Kurtoglu, V. Presser, et al., Adver. Mater. 23 (2011) 4248–4253.
[18] T. Xu, J. Wang, Y. Cong, et al., Chin. Chem. Lett. 31 (2020) 1022–1025.
[19] G. Peng, L. Xing, J. Barrio, et al., Angew. Chem. Int. Ed. 57 (2018) 1186–1192.
[20] M. Zhu, L. Zhang, S. Liu, et al., Chin. Chem. Lett. 31 (2020) 1961–1965.
[21] T. Cai, D. Liu, N. Li, et al., Appl. Catal. B: Environ. 239 (2018) 545–554.
[22] D. Liu, D. Chen, N. Li, et al., Angew. Chem. Int. Ed. 59 (2020) 4519–4524.
[23] J. Zhum, S. Kim, L. Mao, et al., J. Am. Chem/ Soc. 139 (2017) 13234–13242.
[24] J. Zhu, Y. Tang, C. Yang, et al., J. Electrochem. Soc. 163 (2016) A785–A791.
[25] C. Peng, X. Yang, Y. Li, et al., ACS Appl. Mater. Interfaces 8 (2016) 6051–6060.
[26] C. Jin, Z. Li, Y. Zhang, et al., Sep. Purif. Technol. 224 (2019) 33–43.
[27] N. Masunga, B.B. Mamba, K.K. Kefeni, Colloid Surf. A 602 (2020) 125107.
[28] G. Li, R. Wang, B. Wang, et al., Appl. Surf. Sci. 517 (2020) 146212.
[29] H. Yu, R. Shi, Y. Zhao, et al., Adv. Mater. 29 (2017) 1605148.
[30] N. Liu, N. Lu, Y. Su, et al., Sep. Purif. Technol. 211 (2019) 782–789.
[31] X. Hu, X. Hu, Q. Peng, et al., Chem. Eng. J. 380 (2020) 122366.
[32] D. Wu, J. Li, J. Guan, et al., Ind. Eng. Chem. Res. 64 (2018) 206–218.